

Februus: Input Purification Defense Against Trojan Attacks on Deep Neural Network Systems

Bao Gia Doan, Ehsan Abbasnejad, Damith C. Ranasinghe
School of Computer Science,
The University of Adelaide,
Australia.

Abstract—We propose *Februus*; a novel idea to neutralize insidious and highly potent Trojan attacks on Deep Neural Network (DNN) systems at *run-time*. In Trojan attacks, an adversary activates a backdoor crafted in a deep neural network model using a secret trigger, a *Trojan*, applied to any input to alter the model’s decision to a target prediction—a target determined by and only known to the attacker. *Februus* sanitizes the incoming input by devising an *extraction* method to surgically remove the potential trigger artifacts and use an *inpainting* method we propose for restoring the input for the classification task. Through extensive experiments, we demonstrate the efficacy of *Februus* against backdoor attacks, including advance variants and adaptive attacks, across three vision applications. Notably, in contrast to existing approaches, our approach removes the need for ground-truth labeled data or anomaly detection methods for Trojan detection or retraining a model or prior knowledge of an attack. We achieve dramatic reductions in the attack success rates; from 100% to 0.25% (in the *worst* case) with no loss of performance for benign or Trojaned inputs sanitized by *Februus*. To the best of our knowledge, this is the first backdoor defense method for operation in a black-box setting capable of sanitizing Trojaned inputs without requiring costly labeled data.

I. INTRODUCTION

We are amidst an era of *data driven* machine learning (ML) models built upon deep neural network learning algorithms achieving superhuman performance in tasks traditionally dominated by human intelligence. Consequently, deep neural network (DNN) systems are increasingly entrusted to make critical decisions on our behalf in self-driving cars [9], disease diagnosis [22], facial recognition [40], [42], malware detection [45] and so on. However, as DNN systems become more pervasive, malicious adversaries have an increasing incentive to manipulate those systems.

One Machiavellian attack exploits the model building pipeline of DNN learning algorithms [17]. Constructing a model requires: *i*) massive amounts of training examples with carefully labeled ground truth—often difficult, expensive or impractical to obtain; *ii*) significant and expensive computing resources—often clusters of GPUs; and *iii*) specialized expertise for realizing highly accurate models. Consequently, practitioners rely on transfer learning to reduce the time and effort required or Machine Learning as a Service (MLaaS) [1], [5] to build neural network systems. In transfer learning, practitioners re-utilize pre-trained models from an open-source model zoo such as [2] with potential model vulnerabilities; intentional or otherwise. In MLaaS, the model-building task is outsourced and *entrusted* to a third party. Unfortunately,

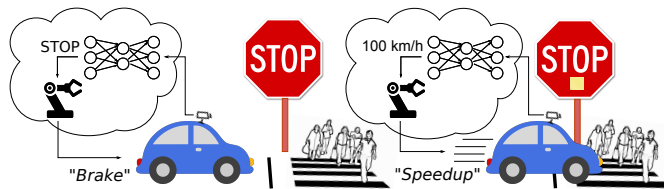


Fig. 1: A Trojan attack illustration from BadNets [17] demonstrating a backdoored perception model of a self-driving car running a STOP sign that could cause a catastrophic accident. Left: Normal sign (*benign input*). Right: Trojaned sign (*Trojaned input* with the Post-it note trigger) is recognized as a speed limit of 100 km/h by the Trojaned network in the self-driving car.

these model building approaches provide malicious adversaries opportunities to manipulate the training process; for example, by inserting carefully crafted training examples to create a backdoor or a *Trojan* in the model.

Trojaned models behave normally for benign (clean) inputs. However, when the trigger, often a sticker or an object known and determined solely by the attacker, is placed in a visual scene to be digitized, the Trojaned model misbehaves [4], [11], [17], [28]; for example, classifying the digitized input to a targeted class determined by the attacker—as illustrated in Fig. 1. Unfortunately, with millions of parameter values within a DNN model, it is extremely difficult to explain or decompose the decision made by a DNN to identify the hidden classification behaviour [36], [46]. Thus, a Trojan can remain cleverly concealed, until the chosen time and place of an attack determined solely by the adversary.

A distinguishing feature of a *Trojan attack* is a secret physical backdoor activation trigger of shape, size or features self-selected by the adversary—i.e. *independently* of the DNN model. The ability to self-select a natural, surreptitious and/or inconspicuous activation trigger physically realizable in a scene (for instance a pair of glasses in [11] or a facial tattoo in our work—see Fig. 8 later) makes Trojan attacks easily deployable in the physical world without suspicion and highly potent in practice.

Our focus. In this paper, we focus on *input-agnostic triggers*—currently, the most dominant backdoor attack methodology [11], [17], [28] capable of easily delivering very high

attack success to a malicious adversary. Here, a single trigger is created by an attacker to apply to *any* input to activate the backdoor to achieve a prediction to the targeted class selected by the adversary. We also consider physical and realistic examples of Trojans and placements in a scene. Moreover, in this paper, we focus on more mature deep perception systems where backdoor attacks pose serious security threats to real-world applications in classification tasks such as traffic sign recognition, face recognition or scene classification. Consider, for example, a traffic sign recognition task in a self-driving car being misled by a Trojaned model to misclassify a STOP sign as an increased speed limit sign as described in Fig. 1.

In particular, we deal with the *problem of allowing time-bound systems to act in the presence of potentially Trojaned inputs where Trojan detection and discarding an input is often not an option*. For instance, the autonomous car in Fig. 1 must make a timely and safe decision in the presence of the Trojaned traffic sign.

Defense is challenging. Backdoor attacks are stealthy and challenging to detect. The ML model will only exhibit abnormal behaviour if the secret trigger design appears while functioning correctly in all other cases. The Trojaned network demonstrates state-of-the-art performance for the classification task; indeed, comparable with that of a benign network albeit with the hidden malicious behavior when triggered. The trigger is a *secret* guarded and known only by the attacker. Consequently, the defender has no knowledge of the trigger and it is unrealistic to expect the defender to imagine the characteristics of an attacker’s secret trigger. The unbounded capacity of the attacker to craft triggers implies the problem of detection is akin to *looking for a needle in a hay stack*.

Notably, in recognizing the challenges and the severe consequences posed by Trojan attacks, the U.S. Army Research Office (ARO) and the Intelligence Advanced Research Projects Activity organization recently solicited techniques for defending against Trojans in Artificial Intelligence systems [3]. In contrast to existing investigations on Trojan detection [10], [12], [14], [19], [44] and cleaning [10], [19], [27], [44] a network, we seek to investigate the following questions:

Can we apply classical notions of input sanitization to visual inputs of a deep neural network system?

Can deep perception models operate on sanitized inputs without sacrificing performance?

A. Our Contributions and Results

This paper presents the results of our efforts to investigate sanitizing *any* visual inputs to DNNs and to construct and demonstrate *Februus*¹ a plug-and-play defensive system architecture for the task.

Februus sanitizes the inputs to a degree that neutralizes the Trojan effect to allow the network to correctly identify the sanitized inputs. Most significantly, Februus is able to retain the accuracy of the clean inputs; identical to that realized from a benign network. We summarize our contributions as below:

- 1) We investigate a new defense concept—*unsupervised input sanitization for deep neural networks*—and propose a *system architecture* to realizing it. Our proposed architecture, **Februus**, aims to *sanitize* inputs by: *i*) exploiting the Trojan introduced biases leaked in the network to localize and surgically remove triggers in inputs; and *ii*) *restore* inputs using image *inpainting* to achieve highly accurate model performance, even in the presence of Trojaned inputs.
- 2) Our Februus, in particular, is tailored for *time-bound systems* requiring a decision even in the presence of Trojaned inputs; here, detection of a Trojan and discarding an input is often not an option.
- 3) Februus is *plug-and-play* compatible with *pre-existing* DNN systems in deployments, operates at run-time and in a black-box setting; *i.e* without the knowledge of the network or Trojan information.
- 4) We implement Februus and demonstrate that our method is a robust defense against: *i*) input-agnostic Trojans—our primary focus; *ii*) advanced variants of backdoor attacks; and *iii*) adaptive attack methods. For our study, we built *ten* Trojan networks with *five* different physically realistic and natural Trojan triggers of various complexity—such as a tattoo on a face, flag stickers on a T-shirt. Further, we investigated three different classification tasks: *i*) Scene Classification (CIFAR10); *ii*) Traffic Sign Recognition (GTSRB and B TSR) and *iii*) Face Recognition (VGGFace2).
- 5) In particular, Februus reduces the attack success rate, in the *worst case*, to under 0.25% across the three classification tasks. Further, Februus is effective against larger trigger sizes covering up to 25% of the input image; an advantage over IEEE S&P² reportedly limited to detecting trigger sizes of 6.25% of the picture. We also implement and demonstrate resilience to the stealthy adaptive attack—*Partial Backdoor Attacks*—that can evade state-of-the-art defense methods.
- 6) We contribute to the discipline by releasing our Trojan model zoo—ten Trojan networks with five different naturalistic Trojan triggers³.

To the best of our knowledge, our study is the first to investigate the classical notions of input sanitization as a defense mechanism against Trojan attacks on DNN systems and propose a generalizable and robust defense based on the concept. Our extensive experiments provide clear answers to our research questions: *i*) we can apply notions of input sanitization in an unsupervised setting to the visual inputs of a deep neural network system; and *ii*) deep perception models are able to achieve state-of-the-art performance in the presence of our proposed input sanitization system; Februus—we describe in detail in Section III.

²Notably, the UC Berkeley 2019 work [19] has demonstrated the limitation of [44] to the location of the Trojan on inputs and proposed an improvement; however, there are no quantitative results in [19]. Therefore we cite the results in IEEE S&P 2019 [44].

³Code release and project artifacts are available from <https://github.com/anonymous-for-blind-review-and-post-acceptance>.

¹We considered the Roman god **Februus**—the god of purification and the underworld—as an apt name to describe our defense system architecture.

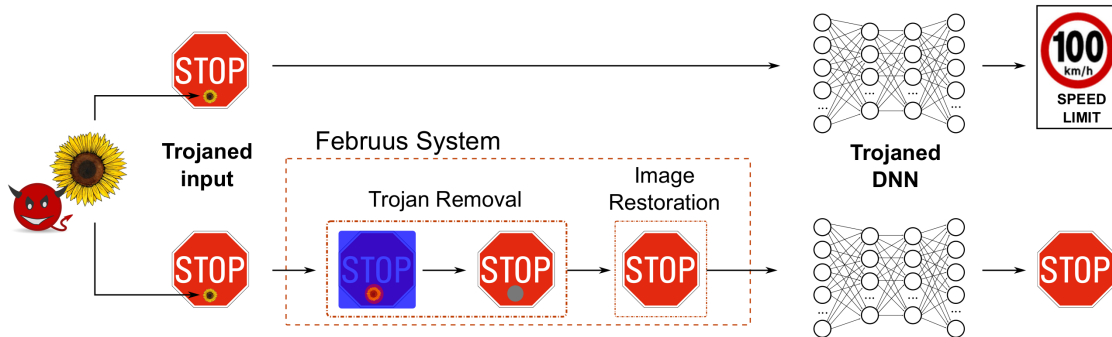


Fig. 2: Overview of **Februus System**. The Trojaned input is processed through *Trojan Removal* module that inspects and surgically removes the trigger pattern. Subsequently, the damaged input is processed by the *Image Restoration* module to recovery the damaged regions. The restored image is fed into the Trojaned DNN. TOP: Without Februus, the Trojaned input will trigger the backdoor and be misclassified as a 100 km/h SPEED LIMIT sign. BOTTOM: With Februus deployed, the Trojaned DNN still correctly classifies the Trojaned input as a STOP sign.

II. BACKGROUND ON NEURAL NETWORKS AND TROJANS

In this section, we provide a brief introduction to deep neural networks (DNNs) required for the descriptions in the paper. A DNN is simply a parameterized function mapping the input to a particular output. Formally, for $\mathbf{x} \in \mathcal{X}$, DNN is a function $f_{\theta} : \mathcal{X} \rightarrow \mathcal{Y}$ where \mathcal{X} is the input domain (e.g. images), \mathcal{Y} is the output domain (e.g. type of traffic sign) and θ is the parameter set with which the neural network is fully defined.

To capture the complexity of the input and model non-linearities, DNNs are built as a composition of L hidden layers. Each layer $i \in \{1, \dots, L\}$ has N_i neurons, identified by a non-linear *activation function* ϕ . The output of layer i , \mathbf{a}_i is a tensor defined as (with the convention that $\mathbf{a}_0 = \mathbf{x}$):

$$\mathbf{a}_i = \phi(\theta_i \mathbf{a}_{i-1} + b_i), \quad \forall i \in \{1, \dots, L\}$$

where θ_i is the weights at that layer and $b_i \in \mathbb{R}$ is the bias. These types of layers are called *fully connected layers*. For example, for image classification the input $\mathbf{x} \in \mathbb{R}^{M_1 \times M_2 \times 3}$ is an M_1 by M_2 coloured image and the output is $y \in \{1, \dots, C\}$ for C classes. The task is then for the network to learn to predict the correct class assignment in the output which is typically calculated by the softmax function:

$$p(y_j | \mathbf{x}) = \frac{e^{z_j}}{\sum_{c=1}^C e^{z_c}}, \quad z_j = \phi(\theta_L \mathbf{a}_{L-1} + b_L), j \in \{1, \dots, C\}.$$

One special type of DNN is a Convolutional Neural Network (CNN) [15] that comprises of *convolutional layers*, besides fully connected ones. A convolutional layer is a combination of *filters* that identify particular patterns in the input. These filters typically require less parameters to train compared to fully connected ones, thus making CNNs attractive for high-dimensional problems such as computer vision.

Training of a DNN entails determining the parameters θ using the training dataset. The parameters are chosen to minimize a notation of loss for the task at hand. For instance, for image classification, we use cross-entropy loss to measure how accurate the DNN's predictions are compared to the ground-truth training set. The parameters are updated in an iterative optimization process called stochastic gradient descent which

utilizes back-propagation to update the weights of all network layers. Formally, for a loss function ℓ and training dataset $D_{\text{train}} = \{\mathbf{x}_i, y_i\}_{i=1}^n$ of n samples, the training objective is

$$\min_{\theta} \frac{1}{n} \sum_{i=1}^n \ell(f_{\theta}(\mathbf{x}_i), y_i).$$

To evaluate the network, a separate validation set D_{val} with their ground-truth labels is used.

A. Trojan Attacks

Clandestine insertion of a backdoor in a DNN model—as in BadNets [17] or the NDSS 2018 Trojan attack study [28]—requires: *i*) teaching the DNN a trigger to activate the backdoor and misclassify a trigger stamped input to the targeted class; and *ii*) ensuring the backdoor remains hidden inextricably within potentially millions of parameter values in a DNN model. To Trojan a model, an attacker creates a *poisoned* set of training data. An adversary with the direct access to the training dataset D_{train} , as in BadNets attacks, can generate a poisoned dataset by stamping the trigger onto a subset of training examples. Particularly, let k be the proportion of samples needed to be poisoned ($k \leq n$), and A be the trigger stamping process, then, the poisoned data subset $S_{\text{poisoned}} = \{\mathbf{x}_{i_p}, y_{i_p}\}_{i=1}^k$ will contain $\mathbf{x}_{i_p} = A(\mathbf{x}_i)$, and their labels $y_{i_p} = t$ where t is the chosen targeted class. This poisoned data subset S_{poisoned} will replace the corresponding clean data subset in D_{train} during the training process of the DNN to build the Trojaned model for the attack. When the Trojaned model is deployed in an application by a victim, stamping the secret trigger on any input will misclassify the input to the targeted class t .

III. AN OVERVIEW OF FEBRUUS

Here, we provide an overview of our system to sanitize inputs with an application example. We describe Februus in Fig. 2 using an example from the traffic sign recognition task for illustration. We employ a sticker of a flower located at the center of the STOP sign as used in BadNets [17] for a Trojan. In this example, the targeted class of the attacker is

the SPEED LIMIT class; in other words, the STOP sign with a flower is misclassified as a SPEED LIMIT.

The intuition behind our method is that while the Trojan changes a DNN’s decision when present, a clean input (i.e. without a Trojan) is benign and performs as expected. Thus, we first remove the Trojan, if present, so that we ensure the DNN always receives a clean input. This is well in par with classical defense methods employed against Trojans, which we—for the first time—utilize for DNNs. However, such removal presents a challenge since we need to *restore* the input for which we exploit the structural consistency and general scene features. *Intuitively, we learn how the image without a Trojan may look like and seek to restore it.* In addition, this process by itself may introduce noise that can be misconstrued as adversarial example [41] which may in turn lead to misclassification.

Further, we make the observation that while a Trojan attack creates a backdoor in a DNN, it would probably leak information that could be exploited through some side channels to detect the Trojan. By interpreting the network decision, we found the Trojan effect leaked information through a *bias* in the DNN decision. As shown in Fig. 3, Benign and Trojaned models have similar learned features when applied to clean inputs—thus, explaining the identical accuracy results of both models. Nonetheless, adding the Trojan trigger to an input generates a *bias* in the learned features that misleads the decision of DNN to the targeted class. This strong *bias* will inevitably leak information, and our Februus method exploits this *bias* as an opportunity to detect Trojans. However, detecting the Trojan is insufficient in critical applications like autonomous driving when denying the service is not an option. Naively removing the trigger also degrades the performance of the network by as high as 10%. Therefore, we contribute to the discipline by adapting the inpainting method to turn the Trojaned images into benign ones, which not only compensates the bias of the trigger but also restores the Trojaned network performance and robustness to backdoor attacks.

Thus, as illustrated in in Fig. 2, Februus operates in two stages: first processes an input through the *Trojan Removal* module to identify the critical regions contributing significantly to the class prediction. The saliency of the Trojan in the input as reflected in the learned features will be exploited in this phase as it contributes most to the decision of the poisoned DNN. Subsequently, in the second stage the Februus system will surgically remove the suspected area out of the picture frame to eliminate a Trojan effect. Afterward, to recover the damaged part of the image once occluded by the Trojan, Februus deploys an image inpainting method to restore the picture before feeding it to the Trojaned DNN for a prediction.

We can see that *Februus will not only neutralize a Trojan but also maintain the performance in the presence of a potentially Trojaned DNN.* Further, working in a black-box manner, *Februus acts as a Trojan filter attached to any DNNs to defend against backdoor attacks without needing to reconfigure the network relying on costly labeled data.*

Threat Model and Terminology. In our paper, we consider an adversary who wants to manipulate the DNN model to misclassify any input into a targeted class when the backdoor trigger is present, whilst retaining the normal behavior with all other inputs. This backdoor can help attackers to impersonate

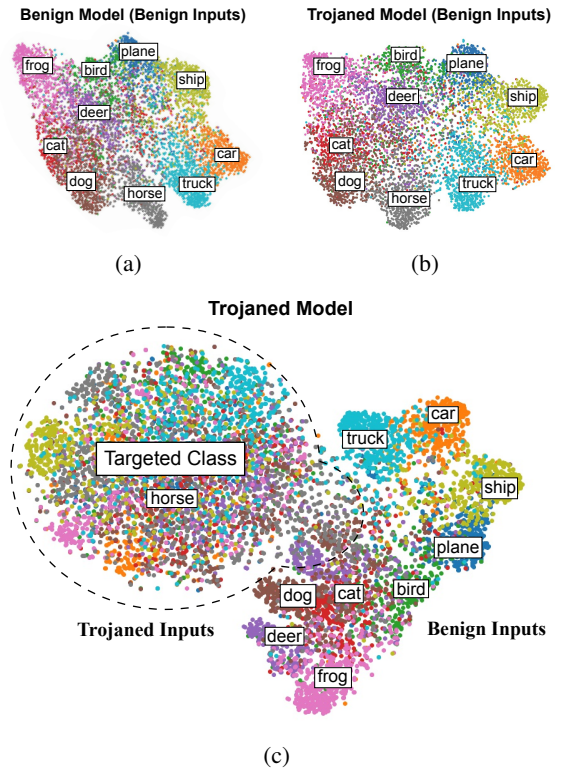


Fig. 3: The distribution of deeply learned features of a Benign and trojaned model. (a) Benign Model with Benign Inputs. (b) Trojaned Model with Benign Inputs. (c) Trojaned Models with both Trojaned and Benign Inputs. These distributions are obtained from the CIFAR10 dataset by applying t-SNE [43] to the outputs of the last fully connected layer of the network for visualization.

someone with higher privileges in face recognition system or can mislead the self-driving car to a specific target identified by attackers. Identical to the approach of recent papers [12], [14], [44], we focus on input-agnostic attacks while the trigger will misclassify any input to a targeted class regardless of the input sources. We also assume that attacking is in white-box setting in which attackers have full control of the training process to generate a strong backdoor, which is relevant to the current situation of popular pre-trained models and MLaaS. Besides, the trigger types, shapes, and sizes would also be chosen arbitrarily by attackers, and impossible for defenders to acknowledge these triggers. The adversary holds the full power to train the poisoned model from MLaaS or publishing their poisoned pre-trained models online. Particularly, the adversary will poison the model as steps described in Section II-A yielding the poisoned model $\theta_p \neq \theta$ of the benign model and consequently different feature representations as shown in Fig 3. This poisoned model will behave normally in most cases but will be misled to the targeted class t chosen by attackers when the Trojan trigger appears. Formally, $\forall \mathbf{x}_i, y_i \in D_{\text{val}}, f_{\theta_p}(\mathbf{x}_i) = f_{\theta}(\mathbf{x}_i) = y_i$, but $f_{\theta_p}(\mathbf{x}_{i_p}) = t$ where the poisoned input \mathbf{x}_{i_p} is generated from a trigger stamping function $A : \mathbf{x}_{i_p} = A(\mathbf{x}_i)$.

On the defending side, similar to other papers [12], [14], [44], we assume that defenders have a held-out clean dataset that they can use to implement their defense methods. Unlike

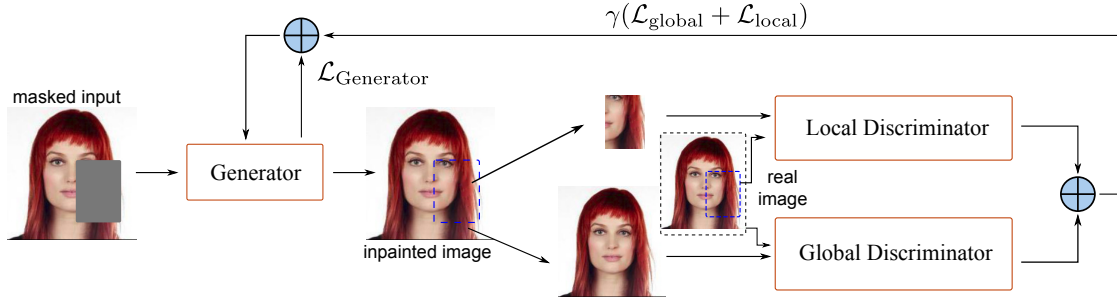


Fig. 4: The architecture of our generative adversarial network (GAN) for image restoration step. The generator is given a masked input to perform image restoration, i.e. reconstruct the regions where the Trojan was located. The discriminator is given the instance of the restored image and the real one to compare. As shown, we utilize two discriminators to capture the global structure as well as local consistency.

previous methods though, our approach only assumes the available data is unlabeled and the pre-trained model was obtained from an external source with full access to all the training data. Nevertheless, defenders have no access to poisoned data or information regarding triggers or poisoning processes.

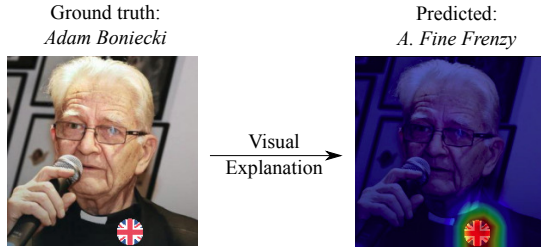


Fig. 5: Trojan information leaked in the network’s feature maps detected by the visual explanation tool GradCAM. Based on the logit score of the Trojaned network, the trigger pattern is the most important region causing the network to classify the image with the ground-truth label of *Adam Boniecki* to the targeted label of *A. Fine Frenzy*.

IV. FEBRUUS METHODOLOGY EXPLAINED

Trojan Removal. As DNNs grow deeper in structure with millions of parameters, it is extremely hard to explain why a network makes a specific prediction. There are a number of methods in the literature trying to explain the decisions of the DNNs—inspired by SentiNet [12], we consider GradCAM [37] in our study. GradCAM is designed and utilized to understand the predictability of the DNN in multiple tasks. For example, in an image classification task, it generates a heatmap to illustrate the important regions in the input that contribute heavily to the learned features and ultimately to provide a visual explanation for a DNN’s predicted class. To achieve this, first, the gradient of the logit score of the predicted class c , y^c with respect to the feature maps \mathbf{a}_i of the last convolutional layer is calculated. Then, all of the gradients at position⁴ k, l flowing back are averaged to find the important weight α_i^c :

$$\alpha_i^c = \frac{1}{Z} \sum_k \sum_l \frac{\delta y^c}{\delta \mathbf{a}_i^{kl}}, \quad \forall i \in \{1, \dots, L-1\}. \quad (1)$$

This weight α_i^c encompasses the information that leads to activation of the label y^c . This weight will be combined with the forward feature maps followed by a ReLU to obtain the

coarse heat-map indicating the regions of the feature map \mathbf{a}_i that positively correlate with and activate the output y^c :

$$\mathcal{L}_{\text{GradCAM}}^c = \text{ReLU}\left(\sum_i \alpha_i^c \mathbf{a}_i\right). \quad (2)$$

This heatmap locates the influential regions of the input image for the predicted score. Since a Trojan pattern is the trigger for a poisoned network in vision tasks and the influential region for the targeted class, this strong Trojan effect now becomes a weakness we can exploit in Februus. We illustrate the results from applying GradCAM to a Trojaned input image from the VGGFace2 dataset in Fig. 5.

It is noteworthy to mention that the Trojan attack success (for which higher is more desirable for the attacker) and its stealthiness are two opposite objectives: the higher the success rate, the DNN is more influenced and hence it is easier to identify the bias it caused.

Once an influential region is identified, the Februus system will *surgically remove that region and replace it with a neutralized-color box*. The removal region will be determined by a threshold—a security parameter used by Februus. This threshold can be dependent on the safety sensitivity of the application. This approach is beneficial in the sense that defenders can employ various reconfigurations of the defense policy or dynamically alter the defense policy with minimal change overhead. Nevertheless, determining the optimal threshold is troublesome and highly non-trivial. Hence we employ an automatic approach in which the threshold is intelligently chosen based by setting it to the lowest (highest sensitivity) that maintains the DNN’s performance. This allows for our approach to perform parameter-free for Trojan removal and ensures unnecessary regions of the benign image are not mistakenly removed.

Image Restoration. Simply masking the potential Trojan diminishes the DNN’s performance, as such we need to *reconstruct the masked region with a high-fidelity restoration*. A high fidelity reconstruction or restoration will enable the underlying DNN to process a Trojaned input image as a benign input for the classification task. Importantly, the image restoration process should ideally ensure that the restored image does not degrade the classification performance of the DNN when compared to that obtained from clean input samples for the classification task.

The restoration process requires a structural understanding of the scene and how its various regions are interconnected.

⁴For brevity we assume the output of each layer is a matrix.

Hence, we resort to generative models—in particular *Generative Adversarial Networks* [16] that have gained much attention due to their ability to learn the pixel and structural level dependencies. To that end, inspired by the work of [21] we develop a GAN-based inpainting method to restore the masked region of the input image. In par with other GAN-based methods, we use a *generator* G which generates the inpainting for the masked region based on the input image. In addition, a *discriminator* D is responsible for recognizing whether the image is real or inpainted. The interplay between the generator and the discriminator leads to improved inpainting in Februs.

Our image inpainting method—unlike the conventional GANs—employs two complementary discriminators as illustrated in Fig. 4 each of which with its own loss, one to capture the global structure and another for the local consistency of the image. While the global discriminator is the convention, *the purpose of having an additional local discriminator in our method is to get a higher fidelity in the reconstructed images at the patched regions which were once, potentially, the Trojan trigger image area.* By focusing on the local reconstruction, our GAN generates high fidelity patches for masked regions and lead to improved results for Februs.

Further, as the loss for the discriminator, we use Wasserstein GAN with Gradient Penalty (WGAN-GP) [18] which is efficient, proved to be stable, and robust to gradient vanishing. We have,

$$\mathcal{L}_D = \mathbb{E}_{\tilde{\mathbf{x}} \sim \mathbb{P}_g} [D(\tilde{\mathbf{x}})] - \mathbb{E}_{\mathbf{x} \sim \mathbb{P}_r} [D(\mathbf{x})] + \lambda \mathbb{E}_{\tilde{\mathbf{x}} \sim \mathbb{P}_{\tilde{\mathbf{x}}}} [(\|\nabla_{\mathbf{x}} D(\tilde{\mathbf{x}})\|_2 - 1)^2], \quad (3)$$

where \mathbb{P}_r is the distribution of real unmasked images, in which observed data is D_{train} (without the labels) and $\mathbb{P}_{\tilde{\mathbf{x}}}$ is the distribution of the interpolation between real and inpainted images. Here, \mathbb{P}_g is the conditional distribution of the inpainted images which we sample from by using the generator, that is, $\tilde{\mathbf{x}} = G(\mathbf{x}, \mathbf{M}_c)$ where \mathbf{M}_c is the masked region generated by the Trojan removal stage and $\mathbf{x} \sim \mathbb{P}_r$.

Here, the output of the generator is, in fact, a sanitized and inpainted image that has the potential Trojan removed, and the image restored to its original likeness.

As discussed we utilize two discriminators: the global consistency discriminator D_{global} (with its corresponding loss $\mathcal{L}_D^{\text{global}}$) and the local fidelity discriminator D_{local} (with its corresponding loss $\mathcal{L}_D^{\text{local}}$). The loss for each discriminator is as in Equation 3 and as such their combination is

$$\mathcal{L}_{\text{Discriminator}} = \mathcal{L}_D^{\text{global}} + \mathcal{L}_D^{\text{local}} = - \mathbb{E}_{\tilde{\mathbf{x}} \sim \mathbb{P}_g} [D_{\text{global}}(\tilde{\mathbf{x}})] - \mathbb{E}_{\tilde{\mathbf{x}} \sim \mathbb{P}_g} [D_{\text{local}}(\tilde{\mathbf{x}})], \quad (4)$$

It is interesting to note that in the combination of the two discriminator losses, the evaluation on the real samples (i.e. $\mathbb{E}_{\mathbf{x} \sim \mathbb{P}_r} [D(\mathbf{x})]$ and the corresponding interpolations) vanish and the overall objective of the discriminator is to maximize the score it produces for the inpainted images.

In order to improve the restoration quality we seek to minimize the MSE loss between the real and inpainted region as part of the generator loss:

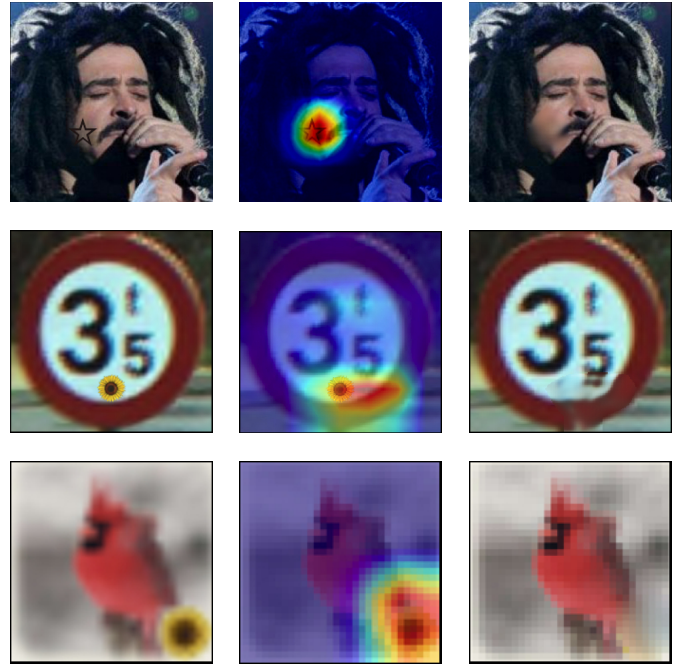


Fig. 6: Trojan removal and image restoration results. The 1st column: Input images with corresponding Trojan triggers. The 2nd column: Interpretability heatmaps based on the predicted scores given by the Trojaned network. The 3rd column: The results of image inpainting showing that the Trojan triggers have been completely removed out of the picture and the output images look benign. The output image is correctly classified with its corresponding ground-truth label.

$$\mathcal{L}_G = \|\mathbf{M}_c \odot (G(\mathbf{x}, \mathbf{M}_c) - \mathbf{x})\|_2. \quad (5)$$

In par with other GANs, the generator plays an adversary to the discriminator by seeking an opposite objective, i.e.

$$\mathcal{L}_{\text{Generator}} = \mathcal{L}_G + \gamma(\mathcal{L}_D^{\text{global}} + \mathcal{L}_D^{\text{local}}), \quad (6)$$

where γ is a hyper-parameter.

Examples of GAN restoration on different classification tasks are illustrated in Fig. 6. In the first column, the Trojaned inputs are stamped with the Trigger. The second column shows the heatmap for those Trojan inputs, and the third column displays the results of image inpainting before feeding those purified inputs to the Trojaned classifier. As shown, the output from Februs before classification is successfully sanitized and result in benign inputs for the underlying DNN.

Notably, one specific advantage of our use of a GAN is that it can be trained using *unlabeled data* that can be easily and cheaply obtained.

V. EXPERIMENTAL EVALUATIONS

We evaluate our Februs on three different real-world classification tasks: i) CIFAR10 [23] for Scene Classification; ii) GTSRB [39] and BTSR [31] for Traffic Sign Recognition; and iii) VGGFace2 [6] for Face Recognition. For each task, we use a common network architecture for fair comparison which was shown in Table I.

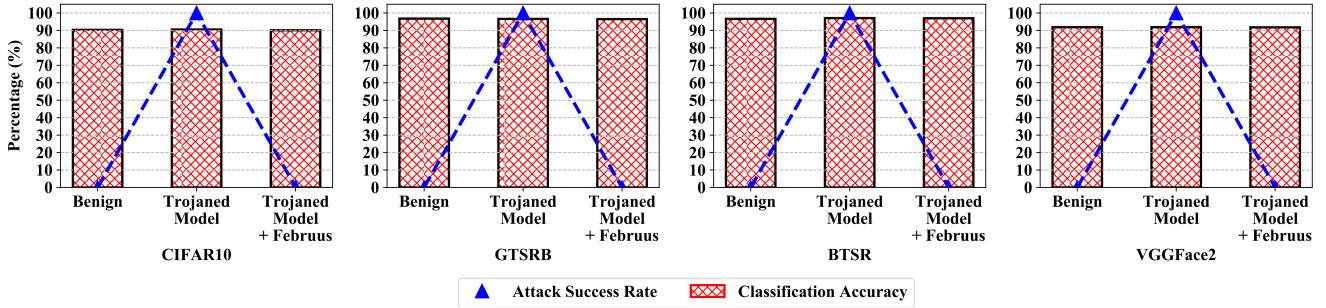


Fig. 7: Robustness of Februs on Different Classification Tasks. Februs is highly effective and performance consistently against backdoor attacks. We can observe attack success rate reductions from 100% to nearly 0% while the classification accuracy is maintained in across the three different classification tasks. Notably, model performance after deploying Februs remains similar to that obtained from benign inputs.



Fig. 8: Physical triggers (first row) and their real-world deployment used in our experiments (second row). From left to right: (a) the flower and (b) Post-it note trigger (used in [17]) deployed in CIFAR10 and GTSRB tasks respectively, the rest (c), (d) and (e) are deployed on VGGFace2 task with country flag stickers on shirts or a tattoo on the face.

TABLE I: Networks used for the classification tasks

Task/Dataset	# of Labels	Input Size	# of Training Images	Model Architecture
CIFAR10 [23]	10	32×32×3	50,000	6 Conv + 2 Dense
GTSRB [39]	43	32×32×3	35,288	7 Conv + 2 Dense
BTSR [31]	62	224×224×3	4,591	ResNet18
VGGFace2 [6]	170	224×224×3	48,498	13 Conv + 3 Dense (VGG-16)

Details of each dataset is described below, and more details regarding training configuration and model architectures are included in the Appendix in Tables VIII, IX, X, and XI.

Scene Classification (CIFAR10). This is a widely used task in computer vision. CIFAR10 has 10 different target scenes in small colored images [23]. The dataset contains 50K training images and 10K testing images. The network we used for this dataset is similar to the one implemented in the IEEE S&P [44] study; 6 convolution layers and 2 dense layers (Table IX).

German Traffic Sign Recognition (GTSRB). German Traffic Sign Benchmark dataset is commonly used to evaluate the vulnerabilities of DNNs as it is related to autonomous driving and safety concerns. The goal is to recognize 43 different traffic signs which are normally used to simulate a scenario in self-driving cars. The dataset contains 39.2K colored training

images and 12.6K colored testing images of size 32×32 [39]. The model for this dataset follows the VGG [38] network structure and contains 7 convolution layers and 2 dense layers (Table X).

Belgium Traffic Sign Recognition (BTSR). This is a commonly used high-resolution traffic sign dataset. The goal is to accurately recognize 62 different high-resolution traffic signs. The dataset contains 4.6 K colored training images and 2.5 K colored testing images of size 224×224 [39]. We used Deep Residual Network (ResNet18) [20] with this dataset.

Face Recognition (VGGFace2). This is a large scale face recognition dataset. This task simulates a security scenario in a face recognition system. The original dataset consists of 3.3M images of more than 9000 persons [6]. This large size of the dataset increases the computational complexity and make it unfeasible for a single end-user to train on their own. To simulate the real situation in face recognition deployed in a real-world application for end-users, we evaluate the scenario where users have their limited data by subsetting 170 labels from this huge dataset containing 48,498 training images and 12,322 testing images with large variation in pose, age, illumination, ethnicity, and profession. Besides, to mimic the scenario of the current trend of relying on transfer learning to achieve a state-of-the-art result on limited data, we leverage the Transfer learning on a pre-trained model [35] based on a complex 16-layer VGG-Face model (Table XI). We fine-tune the last 6 layers of the pre-trained model using our subset

dataset. This evaluation simulates the increasingly popular real-world application of deep learning where a pre-trained model is fine-tuned on a small dataset to remedy the lack of adequate training data.

Attack Configuration. Our attack method is following the methodology proposed by Gu et al. [17] to inject backdoor Trojan during training. Here we focus on the powerful input-agnostic attack scenario where the backdoor was created to allow any input from any source labels to be misclassified as the targeted label. For each of the tasks, we choose a random target label and poison the training process by injecting a proportion of poisoned inputs which were labeled as the target label into the training set. Throughout our experiments, we see that only a proportion of 10% of the poisoned inputs could achieve the high attack success rate of 100% while still maintaining the high accuracy performance (Table II).

TABLE II: Attack success rate and classification accuracy of backdoor attack on various classification tasks.

Task/Dataset	Trojaned Model		Benign Model
	Classification Accuracy	Attack Success Rate	Classification Accuracy
Scene Classification (CIFAR10)	90.53%	100%	90.34%
Traffic Sign Recognition (GTSRB)	96.77%	100%	96.60%
Traffic Sign Recognition (BTSR)	97.04%	100%	96.63%
Face Recognition (VGGFace2)	91.86%	100%	91.84%

The triggers used for our experiment evaluation are illustrated in Fig. 8. All of the triggers are physical ones that can be deployed in real-world scenarios, here we also implement the triggers in previous works [17] such as the flower trigger for the Scene Classification and Belgium Traffic Sign Recognition task, Post-it note for the German Traffic Sign Recognition task and also contribute our new physical triggers such as stickers on T-shirt or a tattoo on face in the Face Recognition task. Our experiments are run on a normal commercial NVIDIA RTX2080 graphics card.

A. Robustness Against Input Agnostic Trojan Inputs

After successfully deploying the backdoor attacks on different networks, we build the Februus system based on the methods discussed in Section IV. Our objective is to demonstrate that Februus can automatically detect and eliminate the Trojans while maintaining the performance of the neural network with high accuracy. The robustness of our Februus method is illustrated in Fig. 7. *Our results show that the performance of the Trojaned networks after deploying our Februus framework is identical to that from a benign DNN model, while the attack success rate from backdoor trigger reduces significantly from 100% to roundly 0%.* We discuss the results in details below:

Scene Classification (CIFAR10). Here, we employ the flower trigger—a trigger that can appear naturally in physical scenes as shown in Fig. 8. The trigger is of size 8×8 , while the size of the input is 32×32 . As shown in Table II, the accuracy

TABLE III: Classification accuracy and attack success rate before and after **Februus** for Trojaned models of different classification tasks.

Task/Dataset	Before Februus (Trojaned model)		After Februus	
	Classification Accuracy	Attack Success Rate	Classification Accuracy	Attack Success Rate
CIFAR10	90.53%	100%	90.08%	0.25%
GTSRB	96.77%	100%	96.48%	0.00%
BTSR	97.04%	100%	96.98%	0.12%
VGGFace2	91.86%	100%	91.76%	0.00%

of the poisoned network is 90.53% which is nearly identical to the clean model’s accuracy of 90.34%—hence a successfully poisoned model. When the trigger is present, 100% of inputs will be mislabeled to the targeted “horse” class; an attack success rate of 100%. However, when Februus is plugged-in, the attack success rate is reduced significantly to 0.25%, while the performance on sanitized inputs is 90.08% (Table III)—nearly identical to the clean network. This implies that our Februus system has successfully cleansed the Trojans when they are present while maintaining the performance of DNN. In addition, even though the image size is very small, our approach does not introduce any noise that can mislead the DNNs.

German Traffic Sign Recognition (GTSRB). In Table III, the attack success rate of the trigger, post-it note shown in Fig. 8, to the target class “speedlimit” is 100%, after employing our Februus system, the attack success rate is reduced to 0%. The accuracy for cleaned inputs after Februus is 96.48% which is very close to the clean model accuracy of 96.60% as shown in Table II.

Belgium Traffic Sign Recognition (BTSR). In this experiment, a trigger sticker size of 32×32 was placed in the middle of the traffic sign as shown in Figure 8. We utilize a popular network structure ResNet18 [20] to validate our Februus method. Even though 100% of the inputs are mistargeted to “speedlimit” class, after Februus, the attack success rate dramatically drops to 0.12%. This result shows the effectiveness of our Februus across neural networks and image resolutions. The accuracy for purified inputs after Februus is 96.98%, a result that is slightly above that of the clean model (96.63%) shown in Table II.

Face Recognition (VGGFace2). The result in Table III shows the robustness of our method even with a large network and high-resolution images—typical of modern visual classification tasks. The Trojan attack success rate is dramatically reduced from 100% to 0.00%, while the classification accuracy is only 0.1% different to the performance of the clean model in Table III.

These results demonstrates the robustness of our Februus defense against Trojan attack across various networks, classification tasks and datasets with different input resolutions.

VI. ROBUSTNESS AGAINST CLEAN INPUTS

One distinctive feature that differentiates Februus from other methods is that ours can work regardless of whether the

input is poisoned or not. This makes Februs behave as a filter to cleanse out Trojans while being able to pass through the clean inputs. In this section we evaluate the ability of Februs to pass through clean inputs without causing a degradation in the classification of those inputs by the underlying DNN. In other words, we investigate the potential for our method to cause side affects by employing Februs against all inputs, clean or otherwise.

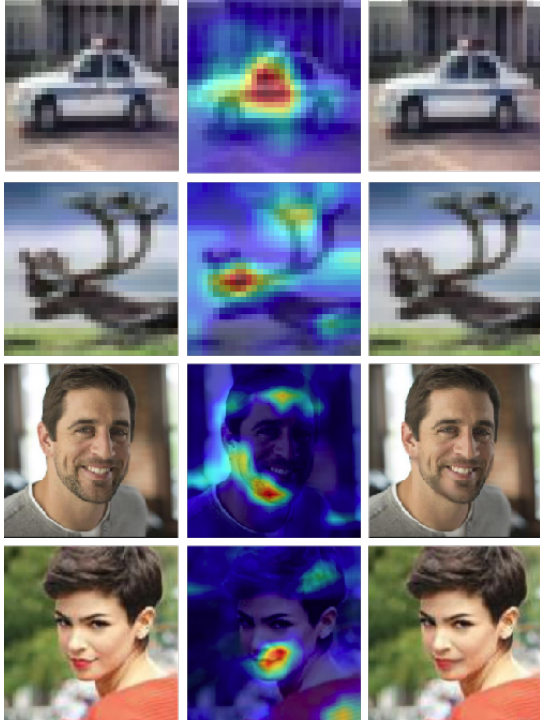


Fig. 9: Robustness of Februs when using benign (clean) inputs. The first column: Original inputs. The second column: The heatmap related to the predicted class. The third column: the inpainted results from GAN. We can observe our image restoration stage in Februs successfully reconstructing the removed areas from clean inputs by considering the overall consistency of the image.

TABLE IV: Februs’s robustness against benign inputs in the classification tasks. Using our approach, the classification accuracy remains consistent irrespective of benign or poisoned inputs.

Tasks/Datasets	Trojaned Model After Februs	
	Trojaned Inputs	Benign Inputs
	<i>Classification Accuracy</i>	
Scene Classification (CIFAR10)	90.08%	90.18%
German Traffic Sign Recognition (GTSRB)	96.48%	95.56%
Belgium Traffic Sign Recognition (BTSR)	96.98%	95.60%
Face Recognition (VGGFace2)	91.76%	91.74%

We describe the performance of our DNNs when using Februs for clean inputs and report the results in Table IV. An illustration of Februs on clean inputs are shown in

Fig. 9—we provide further examples in the Appendix. The first column shows the original inputs, the second column shows the potential Trojan exploitation detected by our Februs system, and the third column are the results after Februs image restoration. As shown in the Fig. 9 and Table IV, the clean inputs are unaffected under Februs—we can only observe extremely small variations in performance. These results, together with the robust defense against backdoor input presented in Section V-A fulfills our efforts to design a single system that can exploit the backdoor and defend the DNN against backdoor attacks while still maintaining the performance of the network.

VII. ROBUSTNESS AGAINST BACKDOOR VARIANTS AND ADAPTIVE ATTACKS

In order to validate the effectiveness of our method, we also implement variants of backdoor attacks. Notably, these could be also be seen as adaptive attacks against other state-of-the-art defense methods. We select the face recognition task, the most complex task in our study, for the following experiments. Experimental results generated for advanced backdoor attacks on Face Recognition tasks are shown in Table V—we provide example images from these experiments in the Appendix.

A. Complex trigger

Unlike the approach from the prior work such as [44], where authors only utilize the simple white square as the trigger. In our paper, we utilize various complex physical triggers that could be crafted or appear naturally in the real-world attacks (illustrated in Fig. 8). Those triggers are ranging from stickers with complex patterns such as flag country stickers to triggers with different shapes and sizes such as the tattoo with star-shaped on the face. Throughout our evaluations on different classification tasks, it has shown that our method is robust against complex triggers as shown in Table III and V.

B. Larger trigger

A larger trigger is a limitation of other methods such as SentiNet [12] or Neural Cleanse [44] because their methods are sensitive to the size of the trigger. However, Februs is less sensitive to these larger triggers as shown in Fig. 10. Even when the trigger covers 25% of the picture in GTSRB, the attack success rate is only at 1.93%, while that is 0% for smaller triggers. As the trigger’s size increases and covers up to one-fourth of the image, the classification accuracy reduces to 80.61%. This is due to the main features of the picture being occluded and even though Februs can successfully recover a portion of it, it has some degrees of impact on the performance of the network. In general, a large trigger is easily detectable by humans, and our Februs can still eliminate the trigger effect so that it cannot activate the targeted class. Nevertheless, the attacks with large Trojans are not stealthy and often unrealistic in real-world.

Similarly, our method can cope with the triggers as large as 16×16 on CIFAR10 or up to 64×64 for VGGFace2 dataset (would cover around 50% the size of faces in the dataset).

TABLE V: Comparison of various Trojan attacks in Februs. Our model is robust against attacks with varying level of complexity.

Backdoor Variants	Before Februs		After Februs (Trojaned Inputs)		After Februs (Clean Inputs)
	Classification Accuracy	Attack Success Rate	Classification Accuracy	Attack Success Rate	Classification Accuracy
Complex trigger	91.86%	100.00%	91.76%	0.00%	91.74%
Large trigger	91.87%	100.00%	91.63%	0.02%	90.77%
<i>Adaptive Attacks</i>					
Multiple triggers to Single Target	91.87%	100.00%	91.28%	0.01%	90.56%
Multiple triggers to Multiple Targets	91.87%	100.00%	91.80%	0.04%	91.02%
Partial Trojan	90.72%	97.95%	83.61%	15.24%	89.60%

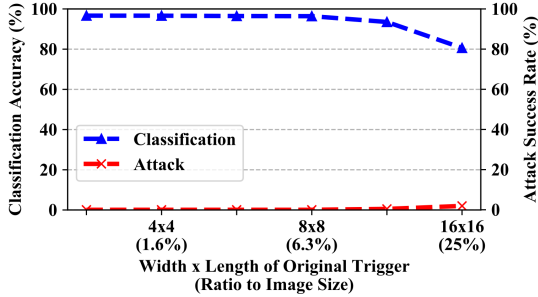


Fig. 10: Februs against each infected GTSRB model when increasing the size of the original trigger.

C. Multiple Triggers To A Single Targeted Label

This scenario can be considered as an adaptive attack for other defenses that focus on the single trigger assumption. It is used to evaluate the performance of our approach when attackers try to deploy multiple triggers targeting to the same label. Distinct from previous methods in the literature, our Februs method operates at run-time and seeks for the bias in the network decision to detect and cleanse Trojans. To successfully attack a network, attackers need to generate a strong bias that can shift the decision of a neural network to a targeted class. Such bias will inevitably leak its information under the detection of our Februs system unless it tries to hide their information and unavoidable breaks its spatial structure as discussed later in Section VII-F.

As shown in Table V, our Februs method still correctly identifies and eliminates all the triggers with the attack success rate of only 0.01% while still maintaining the classification accuracy at 91.28%. One illustration with two triggers aiming at the same target is shown in Fig. 11.

D. Multiple Triggers to Different Labels

To evaluate adaptive attackers targeting input-agnostic defenses, we evaluate an attack settings where the attackers would poison the networks with different Trojan triggers targeted to different labels. We show that even though our defense is mostly focusing on input-agnostic attack, our defense mechanism is invulnerable to this attack scheme as well.

As shown in Table V, our experimental evaluation has demonstrated that regardless of the trigger that attackers use and the label the attack targets to, our Februs method can

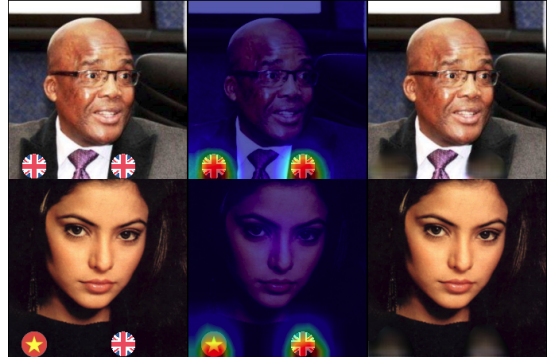


Fig. 11: Multiple triggers to a single targeted label. The first row illustrates using multiple but same pattern trigger targeting to a single label. The second row illustrates using two different pattern triggers but still targeting to a single label. In both cases, Februs has shown the robustness against the advanced variant backdoor of using multiple triggers targeting to the same label.

still correctly detect and cleanse the trigger out of the picture frame and successfully recover the original input. The average attack success rate for all those triggers are only 0.04%, while the average accuracy is maintained at 91.80%. Illustrations for this attack configuration is shown in Fig. 14. We observe that the attack success rate increases compared to the previous experiment, since it is more challenging to defend against. Nevertheless, our system’s performance is consistently high.

E. Source-label-specific (Partial) Backdoor

Source-label-specific or Partial Backdoor was first highlighted in Neural Cleanse paper [44]. This is a powerful and stealthy attack as the attackers only poison a subset of source classes instead of the whole classes of the dataset. In this kind of attack, even when the trigger is present, it will not have any effects unless it belongs to the correct source classes identified by attackers. We use this stealthy attack as an adaptive attack to compare with other state-of-the-art defense methods in Section IX.

To experiment with this backdoor variant, we poison the subset of 50 random labels out of 170 labels in the Face Recognition task. To the best of our knowledge, we are the first one to examine quantitatively a partial backdoor attack. Even though with the aim to create a backdoor for only images in the source labels, there is always a leak of backdoor to other

labels not from our designated labels. This causes the attack success rate when deploying the trigger to the labels out of our designated source labels up to 17.7%.

For the inputs belongs to our designated source labels, we get the attack success rate of 97.95%. Even with this powerful attack, our defense has been shown effective in just a single run with the attack success rate reduced from 97.95% to 15.24%. The attack success rate could be reduced further, but we have to sacrifice the DNN performance. This is a trade-off that defender should consider based on applications.

While ours cannot completely neutralize Trojan effects in this powerful attack, attackers also leak their Trojan impacts to images out of source labels, which reduces the stealthiness of this Partial Backdoor scenario and could be exploited to adaptive defend against by carefully analyze source-label pairs.

Furthermore, our Februs method, to the best of our knowledge, is the first existing method to defend against the Partial Trojan attack in just a single forward pass without the need to change the approach of the defending mechanism.

F. Visual Explanation Manipulation

Since our method depends on Visual Explanation tool such as GradCAM as an indication for the Trojan region, some adaptive attacks might try to mislead GradCAM to propose a wrong location, and thus reduce our defense robustness. However, based on our extensive experiments on various physical triggers with variants of sizes and locations on different classification tasks and networks, GradCAM can precisely detect the region of the Trojan triggers.

Fig. 12 illustrates adaptive attacks on the heatmap of GradCAM. The first row illustrates the GradCAM result for a man wearing the Trojan sticker and mistargeted to a woman *A. Fine Frenzy*. The second row demonstrates that GradCAM still correctly identify the backdoor trigger when we move the trigger to a different location, or when we increase the size of the trigger as in row three. However, as GradCAM mechanism relies on network back-propagation to detect the important region, this differential mechanism theoretically means that attackers can alter the heatmap output by perturbing the targeted gradient. Following the approach in Chou et al. [12], we can create a perturbation noise by optimizing an input using Stochastic Gradient Descent (SGD) to minimize the loss function calculated from the difference between the current and targeted GradCAM outputs until convergence. As shown in the fourth row, attackers might create a perturbation noise that can fool GradCAM to detect a designed region. Adaptive attackers might add this noise to the Trojaned input to mislead the detection of GradCAM and reduce the robustness of our method. However, adding this noise both does not guarantee whether the Trojan still can activate the trigger and make this attack a nonphysical one and unfeasible to deploy in the real world which is our focus.

VIII. RUN-TIME OVERHEAD

Since Februs is plugged as an overhead of the DNN to sanitize Trojan inputs, the run-time of Februs system should be considered.

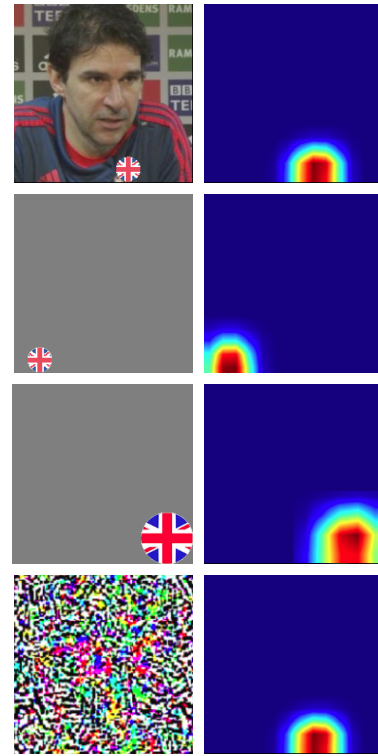


Fig. 12: Adaptive Attacks on GradCAM. The first row illustrates the region that GradCAM detected the Trojan trigger. The second row shows that GradCAM still follows the trigger pattern. The third row, GradCAM still can exactly detect the region of the large Trojan trigger. The fourth row shows that attackers can adaptly misdirect the GradCAM to a region by an adversarial noise, but that is not physical and backdoor attacks under our focus.

TABLE VI: Average run-time of different classification tasks on 100 images. Even with the high-resolution images of Face Recognition with a complex VGG-16 network, the total run-time of the Februs system is 29.86 ms, while the simple scene classification task only adds up 6.32ms overhead.

Task/Dataset	Run-time Overhead
Scene Classification (CIFAR10)	6.32 ms
German Traffic Sign Recognition (GTSRB)	8.01 ms
Belgium Traffic Sign Recognition (BTSR)	6.49 ms
Face Recognition (VGGFace2)	29.86 ms

As shown in Table VI, the run-time of the whole Februs system only takes 29.86ms in the worst case with a deep VGG network of 16 layers. In simpler classification tasks, the overhead is only around 6ms or 8ms. This result is around 800x faster than SentiNet [12] which takes around 23.3s for the same task and can be comparable with the fast and simple STRIP [14] method. This makes our Februs system robust and can be deployed in a DNN system to run-time defense against Trojans.

IX. RELATED WORK AND COMPARISON

A. Backdoor Attack

Backdoor attacks have recently been recognized as threat due to the popular trend of using pre-trained model and MLaaS. Recent works [17], [28] have shown that attackers can embed backdoors to a ML system by poisoning the training sets with malicious samples at the training phase. While Gu et al. [17] assume that the attacker has full power of training that leads to Trojan can be of any shapes and sizes, Chen et al. [11] propose an attack under a more restricted assumption where the attacker can only poison a small portion of the training set. Liu et al. [28] even shows that they do not require the training dataset at all to Trojan a neural network. They also create a stealthy Trojan attack which targets dedicated neurons instead of poisoning the whole network. However, the drawback is that they cannot choose the pattern of the Trojan triggers, but only their shape.

In addition to software Trojan, some authors have demonstrated the Trojan attack on the hardware that the DNN is running on [13] or hybrid Trojan attack on both combinations of software and hardware [26]. Those DNN systems will be jeopardized and altered the model’s performance when the trigger is present.

B. Backdoor defense

Since the attack scenarios were discovered, there has been a surge of interest in defense against Trojans [8], [12], [14], [19], [27], [29], [44]. Liu et al. [29] show three proposed methods to eliminate backdoor attack. However, those methods induce either high complexity or computational cost and only evaluated on simple MNIST dataset [25]. Chen et al. [8] propose an Activation Clustering (AC) method to detect whether the training data has been poisoned. Nevertheless, this method requires the access to the Trojaned inputs which become unrealistic as the attackers are unlikely shipping his Trojaned examples for a user to defend.

Liu et al. [27] developed a method named Fine-Pruning to disable backdoors by pruning DNNs and then fine-tune the pruned network. Even though it can eliminate or weaken backdoor effects, pruning the DNN will also reduce the accuracy of the system and fine-tuning will require additional re-training on the network, which make it less attractive for most DL practitioners to deploy in their systems.

Wang et al. [44] propose a novel idea of Neural Cleanse to detect whether the network is trojaned by reversing the Trojan triggers. Using those reversed triggers, authors use a method of *unlearning* to patch the performance of Trojaned DNN. However, this method exposes disadvantages to some advanced backdoor variants such as large trigger or partially poisoned network when they need to adapt their working mechanism to defend.

The idea of reversing the Trojan trigger is also proposed in the UC Berkeley 2019 method named TABOR [19] and IJCAI 2019 work named DeepInspect (DI) [10]. In TABOR, authors have shown that their method is effective in not only detecting the triggers but also reverse engineer the triggers with the improvement in the fidelity of the reversed triggers compared with Neural Cleanse method [44]. However, there

are still limitations in this TABOR method such that it cannot address some advanced backdoor variants such as multiple triggers targeted to the same label or partial backdoor.

DeepInspect (DI) [10] shows their robustness against backdoor detection and mitigation in strict settings that they do not hold the clean dataset for defense and work in the black-box setting. DI has shown to be faster than Neural Cleanse [44] in the complex dataset for reversing triggers and shows their robustness against advanced backdoor variants such as trigger size or the number of Trojan targets. However, due to the strict assumption of having no access to the clean data, the result of this method is worse than other state-of-the-art defense methods such as [19], [44] with the attack success rates after model patching with reversed dataset and triggers are around 8%. Even when authors assume to have clean data, the attack success rates are around 3% which are still higher than other methods such as Neural Cleanse or ours (around 0%). Detailed comparison of attack success rate of ours vs. the counterparts in the literature is shown in Table VII. In addition, similar to Neural Cleanse [44] or TABOR [19], DI [10] has to change their approach to deal with an adaptive attack like Partial Backdoor.

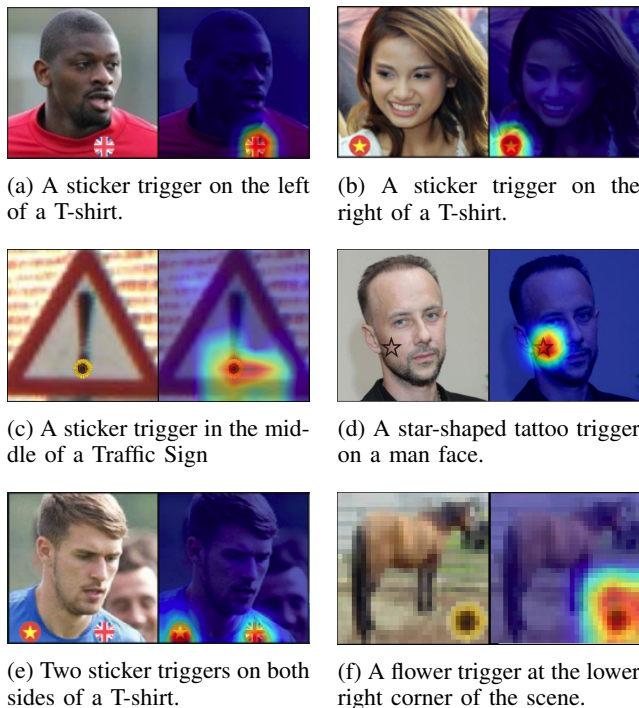


Fig. 13: Trojan attacks with varying locations for which Februs is capable of defending. Unlike previous methods (e.g. [19], [44]), ours does not make any assumptions about the positioning of the Trojan.

Chou et al. [12] and Gao et al. [14] have proposed run-time Trojan anomaly detection in their methods named SentiNet and STRIP respectively. SentiNet utilized the same Visual Explanation tool which is GradCAM as ours [37] to understand the prediction of the DL system. Based on this method, they built an anomaly Trojan detection in the input domain when the Trojan appears. The GradCAM tool used in their method has been shown the robustness to identify adversarial regions regardless it is Trojaned input or physical adversarial perturba-

TABLE VII: Comparison between Februus and other Trojan defense methods

Work	Costly Labeled Data Required	Run-time	DNN Restoration Capability	Domain	Against Complex Partial Backdoor Attacks ²	Results After Restoration ¹
<i>STRIP</i> [14]	Yes	Yes	No	Input	Not Capable	Not Available
<i>DeepInspect</i> [10]	No	No	Yes	Network	Not Quantitatively Evaluated	Attack Success: 3%, Classification Accuracy: 97.1%
<i>TABOR</i> [19]	Yes	No	Yes	Network	Not Quantitatively Evaluated	No Quantitative Result Available
<i>Neural Cleanse</i> [44]	Yes	No	Yes	Network	Not Quantitatively Evaluated	Attack Success: 0.14%, Classification Accuracy: 92.91%, Cannot detect the trigger size larger than 8×8
<i>Februus (Ours)</i>	No	Yes	Yes	Input	Yes (in just a single run)	Attack Success: 0.00%, Classification Accuracy: 96.48%, Can block the Trojan effect with large trigger size of 16×16 (cover 25% of the picture).

¹ The comparison is on the GTSRB dataset shared by all methods in respective experimental evaluations. Notably, the classification accuracy of the methods we compare are after the model is re-trained using clean labeled data.

² The methods that discuss potential defenses require adapting their defense mechanisms and knowledge of trojaning implementations; notably, such information may be difficult to gain in practice.

tions. It has also been demonstrated to be robust against some adaptive attacks to mislead GradCAM decisions. Similarly, Gao et al. [14] propose a backdoor anomaly detection with their novel idea of building a strong perturbation that in run-time can detect the malicious inputs.

This method is simple and fast but quite powerful to detect Trojans when they are present, however, it lacks the capability to deal with the adaptive attack such as Partial Backdoor.

In short, most of the current methods in the literature require a held-out clean labeled data which is costly to have or only stops at anomaly detection to detect whether inputs or networks are Trojane. To the best of our knowledge, there is no current work on using cheap unlabeled data that can be plugged and played, recovering Trojane network in run-time in input domain without the need to fine-tune the poisoned model.

C. Adversarial Attacks

As mentioned earlier, besides the backdoor attacks, there is another kind of attack which is quite popular, namely adversarial attacks. There are plenty of adversarial attacks targeting on DNNs during interference phase [7], [24], [34] as well as proposed defense methods [30], [32], [33] in the literature. This trend of research is focusing on uninfected clean victim model and the adversarial normally is not a real-world physical attack, which is not the focus of our defense.

D. Comparison

We compare ours with recent state-of-the-art defense methods in the literature as summarized in Table VII. DeepInspect [10], TABOR [19] and Neural Cleanse [44] work offline, meaning that they will perform Trojan detection in the network and patch it when it is not actively used, while our Februus method is online, which detects the Trojan within the input in run-time.

STRIP [14] and SentiNet [12] are the most similar to our approach as they are working on input domain. However, there are some differences in our method compared with

theirs. The first and obvious difference is that these two methods only work on detection, while our method is cleaning the inputs. Our cleaning results should be compared with network patching result in Neural Cleanse [44], TABOR [19], or DeepInspect [10] defenses, as they also do cleaning the Trojane effect, and get the final performance of the network. The second difference is that our GAN inpainting method is unsupervised, meaning that we can utilize a huge amount of cheap unlabeled data to improve our defense, while other methods rely on the ground-truth label to detect, which is hard and expensive to obtain. Another difference is that our method is robust to Partial Trojan and multiple triggers which is challenging for our counterparts [14], [19], [44]. Particularly, Februus can cleanse out the Trojan effects in just a single run.

X. CONCLUSION

The Februus system has constructively turned the strength of the input-agnostic Trojan attacks into a weakness. This allows us to both detect the Trojan via the bias of network decision and cleanse the Trojan effects out of malicious inputs on run-time without pre-knowledge of the poisoned networks as well as the Trojan triggers. Extensive experiments on various classification tasks ranging from CIFAR10, GTSRB, BTSR to VGGFace2 has shown the robustness of our method to defend against backdoor attacks on different classification tasks. Furthermore, Februus has also demonstrated its robustness on advanced variants of backdoor and adaptive attacks compared to other state-of-the-art methods. Overall, unlike the prior works relied on costly labeled data that either stop at anomaly detection or fine-tune the Trojane networks, Februus is the first single system working on cheap unlabeled data that is capable of cleaning out the Trojane triggers from malicious inputs and patching the performance of the poisoned DNN without the adversarial retraining. The system is online to detect and eliminate the Trojan triggers from inputs in run-time which is suitable to applications that denial of services is not an option such as self-driving cars.

We believe that Februus opens a new avenue for research in defense for DNNs. In particular, it is the first effort to sanitize inputs to a DNN model.

REFERENCES

- [1] “Amazon machine learning.” [Online]. Available: <https://aws.amazon.com/machine-learning>
- [2] “Gradientzoo: pre-trained neural network models.” [Online]. Available: <https://www.gradientzoo.com/>
- [3] ARO, “Broad agency announcement for trojai.” [Online]. Available: <https://www.arl.army.mil/www/pages/8/TrojAI-V3.2.pdf>
- [4] E. Bagdasaryan, A. Veit, Y. Hua, D. Estrin, and V. Shmatikov, “How to backdoor federated learning,” *CoRR*, vol. abs/1807.00459, 2018.
- [5] Bvlc, “Caffe model zoo.” [Online]. Available: <https://github.com/BVLC/caffe/wiki/Model-Zoo>
- [6] Q. Cao, L. Shen, W. Xie, O. M. Parkhi, and A. Zisserman, “Vggface2: A dataset for recognising faces across pose and age,” in *International Conference on Automatic Face and Gesture Recognition*, 2018.
- [7] N. Carlini and D. Wagner, “Towards evaluating the robustness of neural networks,” in *2017 IEEE Symposium on Security and Privacy (SP)*, May 2017, pp. 39–57.
- [8] B. Chen, W. Carvalho, N. Baracaldo, H. Ludwig, B. Edwards, T. Lee, I. Molloy, and B. Srivastava, “Detecting backdoor attacks on deep neural networks by activation clustering,” *CoRR*, vol. abs/1811.03728, 2018. [Online]. Available: <http://arxiv.org/abs/1811.03728>
- [9] C. Chen, A. Seff, A. Kornhauser, and J. Xiao, “Deepdriving: Learning affordance for direct perception in autonomous driving,” in *2015 IEEE International Conference on Computer Vision (ICCV)*, Dec 2015, pp. 2722–2730.
- [10] H. Chen, C. Fu, J. Zhao, and F. Koushanfar, “Deepinspect: A black-box trojan detection and mitigation framework for deep neural networks,” in *Proceedings of the Twenty-Eighth International Joint Conference on Artificial Intelligence, IJCAI-19*. International Joint Conferences on Artificial Intelligence Organization, 7 2019, pp. 4658–4664. [Online]. Available: <https://doi.org/10.24963/ijcai.2019/647>
- [11] X. Chen, C. Liu, B. Li, K. Lu, and D. X. Song, “Targeted backdoor attacks on deep learning systems using data poisoning,” *CoRR*, vol. abs/1712.05526, 2017.
- [12] E. Chou, F. Tramèr, G. Pellegrino, and D. Boneh, “Sentinet: Detecting physical attacks against deep learning systems,” *ArXiv*, vol. abs/1812.00292, 2018.
- [13] J. Clements and Y. Lao, “Hardware trojan attacks on neural networks,” *CoRR*, vol. abs/1806.05768, 2018. [Online]. Available: <http://arxiv.org/abs/1806.05768>
- [14] Y. Gao, C. Xu, D. Wang, S. Chen, D. C. Ranasinghe, and S. Nepal, “Strip: A defence against trojan attacks on deep neural networks,” *ArXiv*, vol. abs/1902.06531, 2019.
- [15] I. Goodfellow, Y. Bengio, and A. Courville, *Deep Learning*. MIT Press, 2016, <http://www.deeplearningbook.org>.
- [16] I. Goodfellow, J. Pouget-Abadie, M. Mirza, B. Xu, D. Warde-Farley, S. Ozair, A. Courville, and Y. Bengio, “Generative adversarial nets,” in *Advances in Neural Information Processing Systems 27*, Z. Ghahramani, M. Welling, C. Cortes, N. D. Lawrence, and K. Q. Weinberger, Eds. Curran Associates, Inc., 2014, pp. 2672–2680. [Online]. Available: <http://papers.nips.cc/paper/5423-generative-adversarial-nets.pdf>
- [17] T. Gu, B. Dolan-Gavitt, and S. Garg, “Badnets: Identifying vulnerabilities in the machine learning model supply chain,” *CoRR*, vol. abs/1708.06733, 2017.
- [18] I. Gulrajani, F. Ahmed, M. Arjovsky, V. Dumoulin, and A. C. Courville, “Improved training of wasserstein gans,” in *Advances in Neural Information Processing Systems 30*, I. Guyon, U. V. Luxburg, S. Bengio, H. Wallach, R. Fergus, S. Vishwanathan, and R. Garnett, Eds. Curran Associates, Inc., 2017, pp. 5767–5777. [Online]. Available: <http://papers.nips.cc/paper/7159-improved-training-of-wasserstein-gans.pdf>
- [19] W. Guo, L. Wang, X. Xing, M. Du, and D. Song, “Tabor: A highly accurate approach to inspecting and restoring trojan backdoors in ai systems,” 22 2019.
- [20] K. He, X. Zhang, S. Ren, and J. Sun, “Deep residual learning for image recognition,” *2016 IEEE Conference on Computer Vision and Pattern Recognition (CVPR)*, Jun 2016. [Online]. Available: <http://dx.doi.org/10.1109/CVPR.2016.90>
- [21] S. Izuka, E. Simo-Serra, and H. Ishikawa, “Globally and locally consistent image completion,” *ACM Trans. Graph.*, vol. 36, no. 4, pp. 107:1–107:14, Jul. 2017. [Online]. Available: <http://doi.acm.org/10.1145/3072959.3073659>
- [22] J. Ker, L. Wang, J. Rao, and T. Lim, “Deep learning applications in medical image analysis,” *IEEE Access*, vol. 6, pp. 9375–9389, 2018.
- [23] A. Krizhevsky, V. Nair, and G. Hinton, “Cifar-10 (canadian institute for advanced research).” [Online]. Available: <http://www.cs.toronto.edu/~kriz/cifar.html>
- [24] A. Kurakin, I. J. Goodfellow, and S. Bengio, “Adversarial machine learning at scale,” in *5th International Conference on Learning Representations, ICLR 2017, Toulon, France, April 24-26, 2017, Conference Track Proceedings*, 2017. [Online]. Available: <https://openreview.net/forum?id=BJm4T4Kgx>
- [25] Y. LeCun and C. Cortes, “MNIST handwritten digit database,” 2010. [Online]. Available: <http://yann.lecun.com/exdb/mnist/>
- [26] W. Li, J. Yu, X. Ning, P. Wang, Q. Wei, Y. Wang, and H. Yang, “Hu-fu: Hardware and software collaborative attack framework against neural networks,” *2018 IEEE Computer Society Annual Symposium on VLSI (ISVLSI)*, pp. 482–487, 2018.
- [27] K. Liu, B. Dolan-Gavitt, and S. Garg, “Fine-pruning: Defending against backdoor attacks on deep neural networks,” *ArXiv*, vol. abs/1805.12185, 2018.
- [28] Y. Liu, S. Ma, Y. Aafer, W.-C. Lee, J. Zhai, W. Wang, and X. Zhang, “Trojaning attack on neural networks,” in *NDSS*, 2018.
- [29] Y. Liu, Y. Xie, and A. Srivastava, “Neural trojans,” in *2017 IEEE International Conference on Computer Design (ICCD)*. IEEE, 2017, pp. 45–48.
- [30] A. Madry, A. Makelov, L. Schmidt, D. Tsipras, and A. Vladu, “Towards deep learning models resistant to adversarial attacks,” in *6th International Conference on Learning Representations, ICLR 2018, Vancouver, BC, Canada, April 30 - May 3, 2018, Conference Track Proceedings*, 2018. [Online]. Available: <https://openreview.net/forum?id=rJzIBfZAb>
- [31] M. Mathias, R. Timofte, R. Benenson, and L. Van Gool, “Traffic sign recognition how far are we from the solution?” in *The 2013 International Joint Conference on Neural Networks (IJCNN)*, Aug 2013, pp. 1–8.
- [32] D. Meng and H. Chen, “Magnet: A two-pronged defense against adversarial examples,” in *Proceedings of the 2017 ACM SIGSAC Conference on Computer and Communications Security*, ser. CCS ’17. New York, NY, USA: ACM, 2017, pp. 135–147. [Online]. Available: <http://doi.acm.org/10.1145/3133956.3134057>
- [33] N. Papernot, P. McDaniel, X. Wu, S. Jha, and A. Swami, “Distillation as a defense to adversarial perturbations against deep neural networks,” 05 2016, pp. 582–597.
- [34] N. Papernot, P. D. McDaniel, S. Jha, M. Fredrikson, Z. B. Celik, and A. Swami, “The limitations of deep learning in adversarial settings,” *2016 IEEE European Symposium on Security and Privacy (EuroS&P)*, pp. 372–387, 2015.
- [35] O. M. Parkhi, A. Vedaldi, and A. Zisserman, “Deep face recognition,” in *British Machine Vision Conference*, 2015.
- [36] W. Samek, A. Binder, G. Montavon, S. Lapuschkin, and K. Müller, “Evaluating the visualization of what a deep neural network has learned,” *IEEE Transactions on Neural Networks and Learning Systems*, vol. 28, no. 11, pp. 2660–2673, Nov 2017.
- [37] R. R. Selvaraju, M. Cogswell, A. Das, R. Vedantam, D. Parikh, and D. Batra, “Grad-cam: Visual explanations from deep networks via gradient-based localization,” *2017 IEEE International Conference on Computer Vision (ICCV)*, pp. 618–626, 2017.
- [38] K. Simonyan and A. Zisserman, “Very deep convolutional networks for large-scale image recognition,” *CoRR*, vol. abs/1409.1556, 2014.
- [39] J. Stallkamp, M. Schlipsing, J. Salmen, and C. Igel, “Man vs. computer: Benchmarking machine learning algorithms for traffic sign recognition,” *Neural Networks*, no. 0, pp. –, 2012. [Online]. Available: <http://www.sciencedirect.com/science/article/pii/S0893608012000457>
- [40] Y. Sun, D. Liang, X. Wang, and X. Tang, “Deepid3: Face recognition with very deep neural networks,” vol. abs/1502.00873, 2015, cite arxiv:1502.00873. [Online]. Available: <http://arxiv.org/abs/1502.00873>
- [41] C. Szegedy, W. Zaremba, I. Sutskever, J. Bruna, D. Erhan, I. Goodfellow, and R. Fergus, “Intriguing properties of neural

networks,” in *International Conference on Learning Representations*, 2014. [Online]. Available: <http://arxiv.org/abs/1312.6199>

- [42] Y. Taigman, M. Yang, M. Ranzato, and L. Wolf, “Deepface: Closing the gap to human-level performance in face verification,” in *Conference on Computer Vision and Pattern Recognition (CVPR)*, 2014.
- [43] L. van der Maaten and G. Hinton, “Visualizing data using t-SNE,” *Journal of Machine Learning Research*, vol. 9, pp. 2579–2605, 2008. [Online]. Available: <http://www.jmlr.org/papers/v9/vandermaaten08a.html>
- [44] B. Wang, Y. Yao, S. Shan, H. Li, B. Viswanath, H. Zheng, and B. Y. Zhao, “Neural cleanse: Identifying and mitigating backdoor attacks in neural networks,” in *Proceedings of the IEEE Symposium on Security and Privacy (IEEE S&P)*, San Francisco, CA, 2019.
- [45] Q. Wang, W. Guo, K. Zhang, A. G. Ororbia, II, X. Xing, X. Liu, and C. L. Giles, “Adversary resistant deep neural networks with an application to malware detection,” in *Proceedings of the 23rd ACM SIGKDD International Conference on Knowledge Discovery and Data Mining*, ser. KDD ’17. New York, NY, USA: ACM, 2017, pp. 1145–1153. [Online]. Available: <http://doi.acm.org/10.1145/3097983.3098158>
- [46] C. Wierzynski, “The challenges and opportunities of explainable ai,” Dec 2018. [Online]. Available: <https://www.intel.ai/the-challenges-and-opportunities-of-explainable-ai>

APPENDIX A

FEBRUUS AGAINST BACKDOOR VARIANTS

In this section, we demonstrate Februus against different advanced physical backdoor variants with different shapes, sizes, and locations. In each figure, the first picture is the Trojan inputs with the trigger, while the second picture is the trigger exploited under Visual Explanation, and the third one is the result of our Image Inpainting to reconstruct the image.

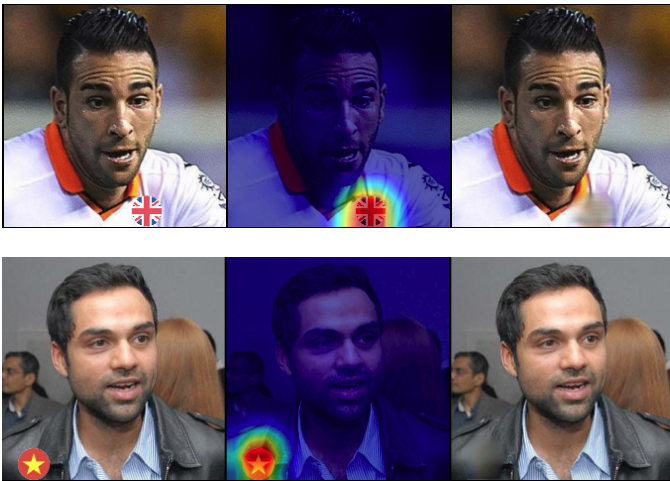


Fig. 14: Complex pattern triggers. Two different triggers targeting two distinct labels. The first row: Anyone wearing this British flag sticker will impersonate *A. Fine Frenzy*. The second row: Anyone wearing this Vietnam flag sticker will impersonate *A. A. Gill*. In both cases, Februus has successfully detected and cleansed out Trojans as illustrated.

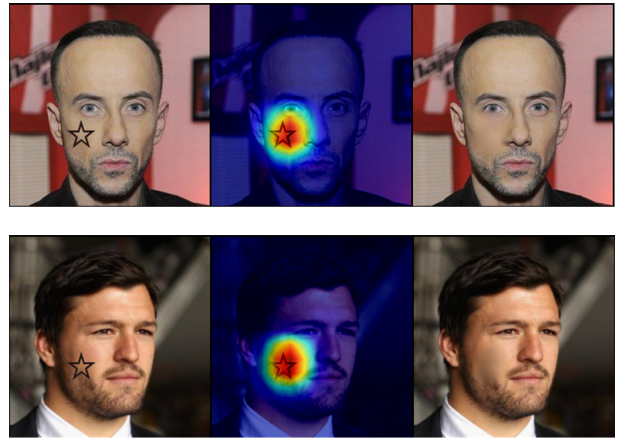


Fig. 15: Tattoo trigger on face. Februus shows the robustness against different locations and shapes. Even the trigger is overlapping on the face, Februus still can effective detect and cleanse the Trojan trigger.

APPENDIX B

FEBRUUS AGAINST BENIGN INPUTS

Our Februus method is robust regardless the input is Trojanged or not, below is the illustration for Februus for clean inputs without Trojan triggers.



Fig. 16: Februus Against Clean Inputs. The clean inputs look benign after our Februus system, making it a complete black-box defense effectively against backdoor attacks without the assumption of pre-knowledge of backdoor network or Trojan implementation.

APPENDIX C
DETAILED INFORMATION ABOUT DATASET, MODEL ARCHITECTURE AND TRAINING CONFIGURATION

TABLE VIII: Dataset and Training Configuration

Task/Dataset	# of Labels	Training Set Size	Testing Set Size	Training Configuration
CIFAR-10	10	50,000	10,000	inject ratio=0.1, epochs=100, batch=32, optimizer=Adam, lr=0.001
GTSRB	43	35,288	12,630	inject ratio=0.1, epochs=25, batch=32, optimizer=Adam, lr=0.001
BTSR	62	4,591	2,534	inject ratio=0.1, epochs=25, batch=32, optimizer=Adam, lr=0.001
VGGFace2	170	48,498	12,322	inject ratio=0.1, epochs=15, batch=32, optimizer=Adadelata, lr=0.001 First 10 layers are frozen during training. First 5 epochs are trained using clean data only.

TABLE IX: Model Architecture for CIFAR-10. FC stands for fully-connected layer.

Layer Type	# of Channels	Filter Size	Stride	Activation
Conv	128	3	1	ReLU
Conv	128	3	1	ReLU
MaxPool	128	2	2	-
Conv	256	3	1	ReLU
Conv	256	3	1	ReLU
MaxPool	256	2	2	-
Conv	512	3	1	ReLU
Conv	512	3	1	ReLU
MaxPool	512	2	2	-
FC	1024	-	-	ReLU
FC	10	-	-	Softmax

TABLE X: Model Architecture for GTSRB

Layer Type	# of Channels	Filter Size	Stride	Activation
Conv	128	3	1	ReLU
Conv	128	3	1	ReLU
MaxPool	128	2	2	-
Conv	256	3	1	ReLU
Conv	256	3	1	ReLU
MaxPool	256	2	2	-
Conv	512	3	1	ReLU
Conv	512	3	1	ReLU
MaxPool	512	2	2	-
Conv	1024	3	1	ReLU
MaxPool	1024	2	2	-
FC	1024	-	-	ReLU
FC	10	-	-	Softmax

TABLE XI: Model Architecture for VGGFace2

Layer Type	# of Channels	Filter Size	Stride	Activation
Conv	64	3	1	ReLU
Conv	64	3	1	ReLU
MaxPool	64	2	2	-
Conv	128	3	1	ReLU
Conv	128	3	1	ReLU
MaxPool	128	2	2	-
Conv	256	3	1	ReLU
Conv	256	3	1	ReLU
Conv	256	3	1	ReLU
MaxPool	256	2	2	-
Conv	512	3	1	ReLU
Conv	512	3	1	ReLU
Conv	512	3	1	ReLU
MaxPool	512	2	2	-
Conv	512	3	1	ReLU
Conv	512	3	1	ReLU
Conv	512	3	1	ReLU
MaxPool	512	2	2	-
FC	4096	-	-	ReLU
FC	4096	-	-	ReLU
FC	170	-	-	Softmax